Measurement of the surface-growth kinetics of reduced $TiO_2(110)$ during reoxidation using time-resolved scanning tunneling microscopy

R. D. Smith,[1] R. A. Bennett,[1,2] and M. Bowker[1,*]
[1]*Centre for Surface Science & Catalysis, Chemistry Department, University of Reading, Reading, United Kingdom*
[2]*Department of Physics, University of Reading, Reading, United Kingdom*
(Received 3 January 2002; revised manuscript received 22 April 2002; published 19 July 2002)

We have employed variable-temperature scanning tunneling microscopy (STM) to follow the kinetics of reoxidation of a nonstoichiometric TiO_2 (110) single-crystal surface. The surface is seen to grow during reoxidation between 573 and 1000 K and at pressures from 5×10^{-8} to 2×10^{-6} mbar O_2. The reaction proceeds by combination of gas-phase O_2 with mobile interstitial Ti^{3+} from the bulk. The surface is observed to grow new layers of TiO_2 in a cyclic process, resulting in the formation of alternate layers of (1×1) and cross-linked (1×2). The growth rate was calculated by measuring the area of new material grown on consecutive STM images of the same area. The rate shows a linear dependence upon oxygen pressure, with an Arrhenius plot indicating an activation barrier of $\sim25\pm4$ kJ mol^{-1} (0.25 ± 0.04 eV/O_2 molecule) for the surface reaction.

DOI: 10.1103/PhysRevB.66.035409 PACS number(s): 68.35.Bs, 68.37.Ef, 68.43.Mn, 68.47.Gh

I. INTRODUCTION

The surfaces of titanium dioxide have attracted a great deal of attention in recent years, due in part to the potential use of TiO_2 as a (photo)catalyst, a light harvesting system for energy production, a gas sensor and its biocompatibility.[1,2] The clean surfaces of rutile have been shown to undergo a complex sequence of reconstructions that are dependent upon sample history and preparation.[3–5] Most recently rutile single crystals have been employed as a support for studies into the behavior of model catalysts produced by deposition of metal nanoparticles on the surface. It has been widely realized that titania is not chemically inert and can react with adsorbates[6–8] or encapsulate supported metal nanoparticles.[9,10] Indeed, considerable reactivity occurs at the surface of bulk reduced single crystals during oxygen exposure at high temperatures. Previously we have reported on the surface restructuring (growth) that occurs during this reoxidation process and confirmed that the process results from the capture of gas-phase oxygen by interstitial titanium ions diffusing out of the bulk.[11,12] However, a greater understanding of the surface-growth kinetics is needed. In this study, the analysis of long sequences of elevated-temperature STM (scanning tunneling microscopy) images taken during reoxidation at various temperatures and pressures provides a different method of extracting surface growth rate data, and hence the reaction kinetics for the rate determining step.

During the preparation of single-crystal titania samples in UHV, the surface Ti:O ratio is altered due to the preferential removal of O from the surface by ion sputtering and vacuum annealing. If the crystal is then annealed to high temperatures, the surface stoichiometry tends to be restored as the high level of surface reduction is spread into the bulk of the crystal. The mechanism for this surface restoration may either be attributed to the dissolution of oxygen vacancies into the bulk concurrent with the transport of oxygen anions to the surface, or to the migration of titanium into the bulk in the form of interstitial ions. The former case was widely cited as the correct mechanism in the literature,[13,14] but recent work by Henderson provides good evidence for the interstitial diffusion mechanism based on isotopic substitution measurements of diffusion using static secondary-ion-mass spectrometry (SSIMS).[15] Studies by ourselves and others show that in fact there is an overwhelming evidence in support of a significant concentration of Ti interstitials in the bulk of ''normally'' prepared crystals.[11,16,17] There appears to be a profound lack of conclusive evidence for the oxygen vacancy model despite its widespread promotion, a point well made by Henderson that seems to have escaped the attention of some of the scientists in this area.

The way in which oxygen is activated is a fundamental problem in oxidation catalysis and especially so in selective oxidation. Often isotopic exchange reactions of oxygen gas molecules with surface atoms are used to investigate the kinetics of activation on metal oxide surfaces.[18] Typically three exchange processes are encountered, denoted by R^0, R^1, or R^2, where the superscript indicates the number of surface oxygen atoms involved, which are described by the following equations:

$$^{18}O_{2(g)} + {}^{16}O_{2(g)} \rightarrow 2\,{}^{18}O{}^{16}O_{(g)}, \quad R^0 \text{ mechanism,} \tag{1}$$

$$^{18}O_{2(g)} + {}^{16}O_{(s)} \rightarrow {}^{18}O{}^{16}O_{(g)} + {}^{18}O_{(s)}, \quad R^1 \text{ mechanism,} \tag{2}$$

$$^{18}O_{2(g)} + 2\,{}^{16}O_{(s)} \rightarrow {}^{16}O_{2(g)} + 2\,{}^{18}O_{(s)}, \quad R^2 \text{ mechanism.} \tag{3}$$

Note that (g) and (s) represent gas phase and surface atoms, respectively.

The R^0 mechanism involves the collision of two gas-phase O_2 molecules without the participation of any surface oxygen. R^1 involves the exchange of one ^{18}O atom from a gas-phase $^{18}O_2$ with a surface ^{16}O atom. R^2 is the exchange of a complete $^{18}O_2$ with two surface ^{16}O atoms resulting in the desorption of a $^{16}O_2$ molecule.

By analyzing the composition of isotopically labeled gas mixtures as a function of time and temperature over various

oxides the rate constants for these processes have been deduced. However, the regrowth mechanism that we have shown to be active for the nonstoichiometric TiO_2 surface cannot be directly reconciled with these processes. Instead oxygen is taken up by the surface by reaction with interstitial ions resulting in the growth of new layers of TiO_2. These new layers will have an oxygen isotope distribution that is representative of the gas phase and may show spatial correlation between the isotopes distributed on the surface as whole molecules become trapped by the interstitials.

The data we present show that the surface growth is sensitive to temperature and pressure. The growth of the surface occurs with low activation energy and, hence, the surface structure and reactivity may be strongly influenced by nonstoichiometry. Such growth effects should be addressed when making kinetic measurements, especially where equilibrium reaction conditions would indicate that the oxide is nonstoichiometric.

II. EXPERIMENT

A W.A. Technology variable temperature STM was employed, and in this work imaging was undertaken at the reaction temperature in a low partial pressure of oxygen. The UHV chamber containing the STM typically had a base operating pressure of 1×10^{-10} mbar. The chamber was equipped with low-energy electron diffraction optics (VG Scientific) that also allowed retarding-field Auger measurements to be made, and an Ar^+ ion sputtering gun. A more detailed description of the chamber facilities may be found elsewhere.[19] Reoxidation experiments were carried out *in situ* by dosing O_2 into the chamber using a fine leak valve. The sample was kept at a constant temperature during reoxidation such that thermal drift was low over the time period of the experiments. This allowed long sequences of images to be taken of nearly the same area. The TiO_2 (110) crystal (PI KEM, UK) was prepared by cycles of room temperature 600 eV Ar^+ sputtering and annealing to 1173 K. This gave a reproducible (1×1) terminated surface but a nonstoichiometric bulk and near-surface region. The degree of nonstoichiometry was indicated by the dark blue color of the TiO_2 crystal.[20]

III. RESULTS AND DISCUSSION

A. STM imaging

Figure 1 shows a sequence of images of the same area taken during reoxidation of a (1×1) bulk terminated TiO_2 (110) surface at 723 K. As the sequence progresses, the growth of successive additional layers of titania is observed. The growth process results from the combination of the gas-phase O_2 with interstitial Ti ions from the nonstoichiometric bulk. This occurs first of all by the growth of nucleation points on top of the (1×1) terraces. The nucleation points act as seeds for (1×2) strings that grow slowly along the $\langle001\rangle$ direction. Once these strings reach an appreciable length and have other (1×2) strings adjacent to them, then cross-linking features appear between the rows. A detailed model of the cross-linked (1×2) has been published elsewhere.[21] Areas of cross-linked (1×2) are subsequently filled in rapidly by (1×1) islands and by the outward growth of the step edges (step-flow growth). The reaction is cyclic and once the new layer of (1×1) has reached an appreciable size, the growth of another layer of cross-linked (1×2) proceeds on top of that. In the following text cross-linked (1×2) shall be referred to as (1×2) for simplicity.

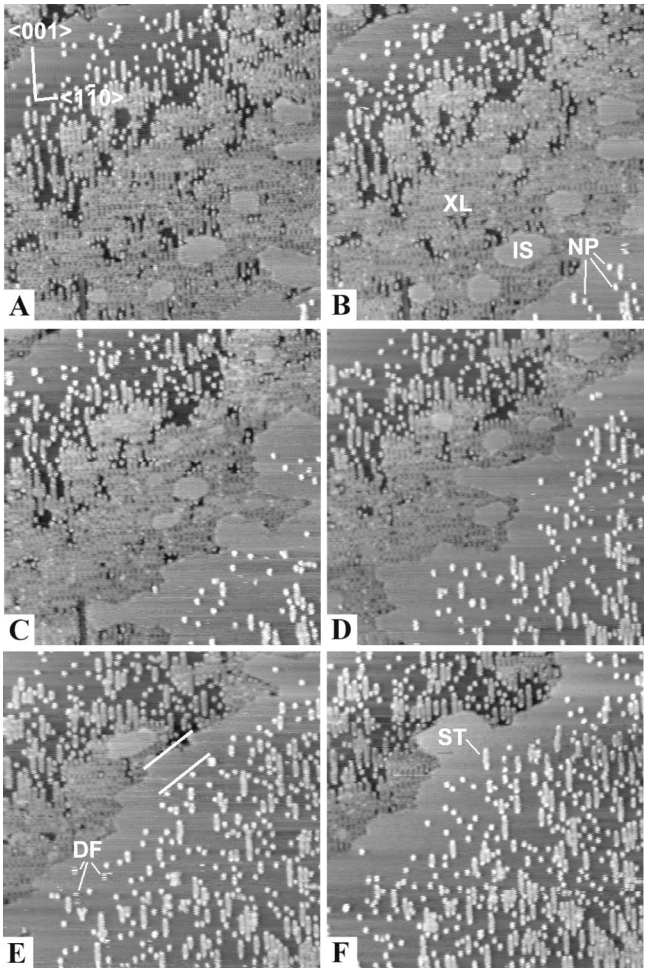

FIG. 1. A sequence of images taken during the reoxidation of the TiO_2 (110) (1×1) surface at an O_2 pressure of 1.0×10^{-7} mbar and a sample temperature of 723 K. All images are 750×750 Å, sample bias: +1.1 V, tunnel current 0.10 nA, constant current imaging. The total oxygen exposures for *A*-*F* were 609, 622, 654, 682, 709, and 750 L, respectively. This equates to a time interval on average of 370 s between these images. Examples of the main features of the images are marked as follows: diffusing features (DF), nucleation points (NP), (1×2) strings (ST), (1×1) islands (IS), area of cross-linked (1×2) (XL). Note also the parallel lines in *E*, these highlight the width of the depletion region adjacent to the step edge, but this can be seen in all of the images in this figure.

Diffusing features are observed on the surface during reoxidation. They are seen particularly when the tip state is favorable, and the row resolution is good. We believe that these features are the precursor species to the nucleation point. They diffuse easily up and down the rows in the $\langle001\rangle$ direction during scanning until they become locked in posi-

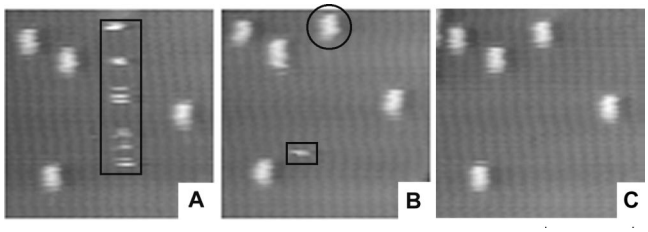

FIG. 2. Three enlarged segments from consecutive images taken 480 s apart during reoxidation of the TiO_2 surface at an O_2 pressure of 1.1×10^{-7} mbar. The surface temperature was 673 K. The image size is 105×105 Å. A diffusing feature is visible within the rectangle in image *A*. In image *B* a new nucleation point has formed (circle) along the $\langle001\rangle$ direction from the diffusing feature in image *A*. The diffusing feature in image *B* (square) does not result in the formation of a new nucleation point in image *C* (even outside the enlarged area). It should be noted that these images are scanned with the fast-scan direction horizontal from the bottom left to the top right.

tion to form a nucleation point (Fig. 2). The example in Fig. 2(a) was seen to diffuse along the $\langle001\rangle$ direction at an observed rate of 6 Å s^{-1}. As diffusion is a random hopping process, the total distance travelled is likely to be significantly greater. In contrast, the nucleation points, once formed, did not diffuse.

The diffusing species may not be easily observed in these experiments due to the time needed to take an STM image (in this case of the order of 1–2 min) compared to the short time period required for diffusion. The appearance of the diffusing species in the images consists of short streaks in the $\langle1\bar{1}0\rangle$ (fast scan) direction of similar width to (1×2) rows. The middle of each streak is centered on the bright row of the (1×1), which is generally accepted to be the fivefold-coordinated Ti row in the trough of the (1×1) structure.[22,23] This shows that the species is diffusing along the troughs. The streaks result from the brief presence of the moving species underneath the tip for the time needed to scan one or two lines of the image. Depending on the direction of diffusion the diffusing species may be observed more than once in the same scan as neighboring streaks along the $\langle001\rangle$ direction. Diffusion in the $\langle1\bar{1}0\rangle$ direction was not observed in these experiments.

It appears that the formation of the diffusing species is not always followed by the formation of a nucleation point [Figs. 2(b), (c)]. The diffusing features are metastable and have a short lifetime on the surface. They may either react further to form a nucleation point, become directly incorporated into an outward growing step edge (this may be what has happened in Fig. 2(c), outside the enlarged area there is a nearby step edge), or it is possible that they can decompose back to gas-phase O_2 and interstitial Ti^{3+}. We tentatively suggest that the diffusing feature may be a TiO_2 species (Fig. 3, left, *A*). Although it is possible that the diffusing species is interstitial titanium that diffuses upwards through the bulk and spends a short time diffusing along the rows on the surface before returning to the bulk, we feel this is unlikely. This is because at the same temperatures, when bulk interstitial Ti^{3+} is mobile, but in the absence of gas-phase O_2, we have never

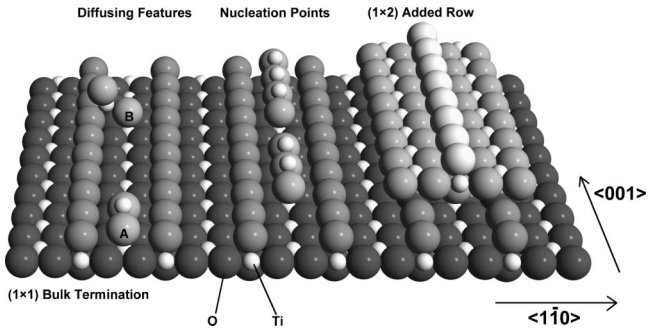

FIG. 3. A model showing the proposed structures of the different features present on the surface at different stages of growth during reoxidation. Two possible structures are proposed for the diffusing features, *A* and *B*. *B* is based on the Elliott and Bates model (Ref. 24).

observed such features. It is also not likely that the species is adsorbed O_2 as oxygen is not normally imaged in the STM on TiO_2. On the (1×1) surface at positive sample bias it is the titanium that appears as bright rows despite the topography. Topographically the oxygen occupies a more elevated position. The contrast of the diffusing species in the STM image in Fig. 2 is very similar to the nucleation points, which leads to the conclusion that the species must be similar in structure but smaller and more mobile, hence TiO_2. An alternative possible structure, based on recent work by Elliott and Bates[24] is also shown in Fig. 3 (marked *B*). This is still a TiO_2 unit but is bound to both the bridging oxygen and the five-coordinate Ti row. In order that this unit should appear to be central on the Ti row in the STM data, it is possible that it may ''flip'' between equivalent states on opposing bridging oxygen rows.

Measurement of the nucleation points in the images in Fig. 1, shows that they are initially ≈11 Å in length in the $\langle001\rangle$ direction. As the nucleation points are such undercoordinated Ti species, they are likely to appear larger in STM images than they are in reality. We therefore suggest that the structure of the nucleation points is simply an extension of the TiO_2 unit of the diffusing feature. Two possible structures are shown in the center of Fig. 3. It is unlikely that nucleation points have the Elliott and Bates structure above because in this structure the Ti is offset with respect to the underlying lattice. We should therefore be able to observe this is in the STM data. Our data consistently show that nucleation points lie directly above the exposed Ti row of the (1×1). It is clear from the data that nucleation points can be considered to be the starting point for (1×2) string growth.

The lack of nucleation points and (1×2) strings adjacent to the step edge on the uppermost terrace is also apparent in Fig. 1. The growth of new nucleation points appears to be limited within a depletion region adjacent to the step edge on the upper terrace. This is especially noticeable in the case of small (1×1) islands; the islands must reach an appreciable size before nucleation can occur on their surface. The depletion region would appear to be smaller for growth at lower temperatures and at higher pressures. Under high-pressure conditions the nucleation of new layers occurs well before the completion of the old ones, resulting in a much rougher

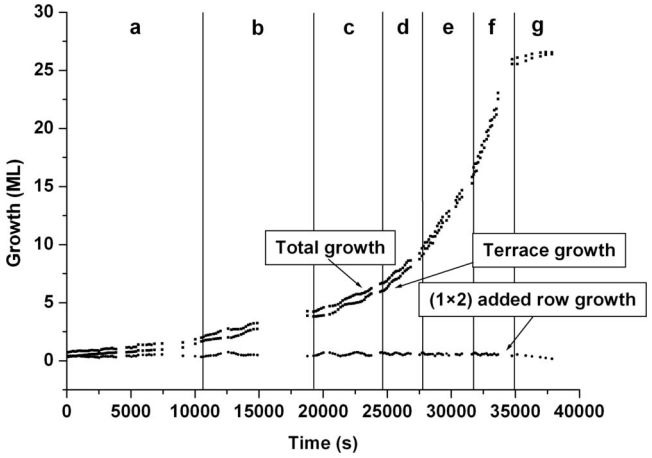

FIG. 4. A plot showing the growth of surface TiO_2 in monolayers against time in seconds from the start of O_2 dosing for the reoxidation sequence in Fig. 1. Each marked segment represents a different pressure of O_2 (mbar) as follows: $a=5.0\times10^{-8}$, $b=1.0\times10^{-7}$, $c=2.0\times10^{-7}$, $d=4.0\times10^{-7}$, $e=8.0\times10^{-7}$, $f=1.6\times10^{-6}$, $g=5.0\times10^{-8}$. Note the small oscillations about a constant value for the (1×2) added row growth, and terrace growth.

surface morphology. Increased surface roughness is expected from a nucleation point of view. High pressure leads to a high coverage of diffusing features, which in turn leads to more rapid nucleation. This kind of depletion region is not unique to the reoxidation reaction on TiO_2. It has also been observed by Iwasawa, Onishi, and Fukui in the distribution of ''product particles'' after heating TiO_2 in formic acid at 450 K.[25] It has been previously reported that diffusion of interstitials beneath the surface is favorable along the channels in the $\langle001\rangle$ direction (C axis) in the rutile structure.[26] Diffusion in the channels could be more favorable than diffusion vertically to the surface. This was suggested by others as a reason for the formation of depletion regions.[17,27] The interstitials may become depleted in the areas adjacent to the step edges as they diffuse towards the edge and capture gas-phase O_2, resulting in step flow growth. We do not believe this to be the case as some other work reports that diffusion is faster perpendicular to the $\langle001\rangle$ channels.[28] Indeed some of our most recent modeling work confirms this.[29] This leads us to suggest that an alternative reason for the depletion regions may be due to the TiO_2 diffusing species being able to step down over step edges, but not being able to step up again.[30] In this case, species that initially form in close proximity to step edges on the upper terrace may step down and become incorporated into the outward growing step edge. This would reduce the probability of nucleation point formation in this region on the upper terrace.

B. Oxidation kinetics

Analysis of the images to obtain the kinetic information was achieved by measuring the area of each terrace individually over successive images. This was combined with the fractional coverage of (1×2) in order to give the overall growth of the surface. An example of the data obtained from a lengthy sequence of images of which just a few are presented in Fig. 1, is shown in Fig. 4. This shows quite clearly that the rate increases for six successive increases in the O_2 pressure. The reproducibility of the data is good, on returning to the original starting pressure 6 h 50 min later a very similar rate is observed (segments *a* and *g*). This is interesting, because it implies that the availability of interstitial titanium ions has remained virtually constant throughout the whole experiment. Plotting the growth rate against O_2 exposure (not shown) instead of time highlights this; a straight line is obtained for the whole experiment. We have not attempted to quantify the concentration of interstitial Ti in the bulk. The color of the crystal provides a very rough ''by eye'' measure, the darker the crystal, the higher the degree of reduction.[20] However, this is not sufficiently accurate as a measure of bulk reduction. The small number of sputtering and annealing cycles between experiments ensured that the variation in reoxidation rate due to any change in interstitial concentration was kept to a minimum.

It is interesting to observe that the fractional coverage of (1×2) rows remains largely constant over a long time period. However, on close observation of the data it is possible to see oscillations in the coverage as well as the terrace and overall growth rates (Fig. 4). These result from the cyclic nature of the surface reaction. Although the (1×2) grows steadily on top of the (1×1) terraces, it never reaches 100% coverage as it is rapidly filled in again to form (1×1), once the (1×2) strings are sufficiently densely packed. It then takes some time for the (1×1) islands to become large enough to support the next layer of (1×2), so the coverage of (1×2) is greatly reduced. The reason that the (1×2) fills in so rapidly is probably not because of increased oxygen sticking probability on the (1×2) surface compared to the (1×1). In fact, the amount of material required to fill the voids in the (1×2) structure to make (1×1) is much smaller than that needed to form the (1×2) in the first place. This is because the (1×2) structure is effectively the same as (1×1) but with a single missing TiO_2 unit in each (1×2) unit cell.[21] The formation of (1×2), which has the stoichiometry Ti_3O_5, requires three such units. The period of the oscillations decreases with increasing O_2 pressure as the increased reaction rate causes the cycle to repeat more rapidly. For example, at 723 K at an O_2 pressure of 2.0×10^{-7} mbar the oscillation period is 2370 ± 100 s. This decreases to 1120 ± 100 s at 4.0×10^{-7} mbar. At the highest pressures, the (1×1) island sizes become so much smaller and nucleation so much faster that the oscillations break down and the (1×2) coverage remains nearly constant.

Rate constants for the reaction at different temperatures were obtained by plotting growth rate against O_2 pressure (Fig. 5). This figure shows the growth rate at two different temperatures for varying pressures of O_2. The rate constants obtained from these plots have units of $\mathrm{ML\,s^{-1}\,mbar^{-1}}$ because they are pseudo-first-order; they assume a constant concentration of Ti^{3+} in the bulk. The rate constant at 723 K is found to be 1.9×10^3 $\mathrm{ML\,s^{-1}\,mbar^{-1}}$. From the limited number of data points at 573 K we can estimate the rate constant at this temperature to be $\sim7\times10^2$ $\mathrm{ML\,s^{-1}\,mbar^{-1}}$.

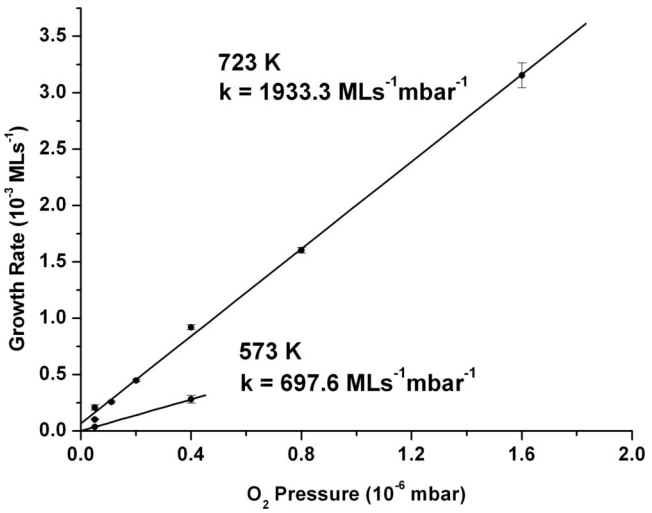

FIG. 5. A plot showing the growth rate in monolayers per second against the O_2 pressure for sets of data taken at two different temperatures, 573 and 723 K. The data were obtained by taking the gradient of the total growth rate in Fig. 4 for each pressure.

Repetition of the reoxidation experiment at five different temperatures has allowed us to produce the Arrhenius plot shown in Fig. 6. It can be seen that the points lie close to a straight line. The activation energy calculated from this line is $25(\pm 4)$ kJ mol^{-1}, a very low value. We shall discuss the reasons for this in the following section.

IV. MECHANISM FOR REOXIDATION

We propose that the following preequilibrium mechanism as a viable one for the reoxidation process:

(1) $Ti^{3+}_{(b)} \rightleftharpoons Ti^{3+}_{(s)}$,

(2) $Ti^{3+}_{(s)} + O_{2(g)} + 3e^- \rightarrow TiO_{2(s)}$ (rate-limiting step),

where (b) denotes bulk, (s) denotes surface, (g) denotes gas.

Although, there are likely to be many more steps in the overall reaction, the formation of a TiO_2 diffusing unit appears to be the precursor to the formation of all structures in the growth process. The formation of this unit must be the rate-determining step as we believe it is the only step that involves gas-phase oxygen.

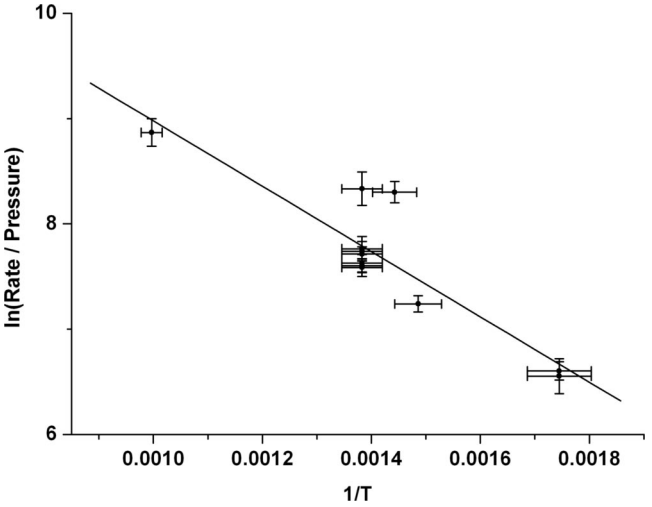

FIG. 6. An Arrhenius plot for growth rate data taken at five different temperatures including the two datasets shown in Fig. 5. Errors in temperature are estimated from previous temperature programmed desorption (TPD) experiments using the same system.

We assume that the concentration of Ti^{3+} at the surface at a particular temperature is constant and small [steady state approximation: (SSA)] and is maintained by a ready supply from the bulk. There is always some Ti^{3+} present on the surface at elevated temperatures whether oxygen is present or not. In the absence of oxygen its lifetime at the surface is very short, in the presence of oxygen it can be trapped by reaction (2). The TiO_2 crystals are electrically conductive so we can assume charge transfer to be rapid. We can therefore write an expression for the rate of formation of TiO_2 as follows:

$$\frac{d[\mathrm{TiO_2}]}{dt} = k_2[\mathrm{Ti}^{3+}_{(s)}][e^-]^3 P_{\mathrm{O_2}}. \tag{4}$$

Invoking the SSA for $[Ti^{3+}_{(s)}]$ in reaction (1),

$$\frac{d[\mathrm{Ti}^{3+}_{(s)}]}{dt} = 0 = k_1[\mathrm{Ti}^{3+}_{(b)}] - k_{-1}[\mathrm{Ti}^{3+}_{(s)}] - k_2[\mathrm{Ti}^{3+}_{(s)}][e^-]^3 P_{\mathrm{O_2}}. \tag{5}$$

It follows that:

$$[\mathrm{Ti}^{3+}_{(s)}] = \frac{k_1[\mathrm{Ti}^{3+}_{(b)}]}{k_{-1} + k_2[e^-]^3 P_{\mathrm{O_2}}}. \tag{6}$$

Therefore,

$$\frac{d[\mathrm{TiO_2}]}{dt} = \frac{k_2 k_1[\mathrm{Ti}^{3+}_{(b)}][e^-]^3 P_{\mathrm{O_2}}}{k_{-1} + k_2[e^-]^3 P_{\mathrm{O_2}}}. \tag{7}$$

However, as the electrons initially resulted from the formation of bulk interstitial Ti^{3+}, we can write: $[e^-] = 3[\mathrm{Ti}^{3+}_{(b)}]$, thus maintaining charge neutrality, and therefore, $[e^-]^3 = 27[\mathrm{Ti}^{3+}_{(b)}]^3$, and substitute this into Eq. (7):

$$\frac{d[\mathrm{TiO_2}]}{dt} = \frac{27 k_2 k_1[\mathrm{Ti}^{3+}_{(b)}]^4 P_{\mathrm{O_2}}}{k_{-1} + 27 k_2[\mathrm{Ti}^{3+}_{(b)}]^3 P_{\mathrm{O_2}}}. \tag{8}$$

If $k_2 P_{\mathrm{O_2}} < k_{-1}$ then the reaction is first order in O_2. The data indicate that this is the case and that $[\mathrm{Ti}^{3+}_{(b)}]$ is constant, so,

$$r = \frac{d[\mathrm{TiO_2}]}{dt} = 27 k_2 k[\mathrm{Ti}^{3+}_{(b)}]^4 P_{\mathrm{O_2}}. \tag{9}$$

By expanding $k_2 K$ into an Arrhenius-type expression we can see that

$$k_2 K = \frac{A_2 A_1}{A_{-1}} e^{-(E_2 + \Delta H)/RT} = A' e^{-E'/RT}. \tag{10}$$

Therefore,

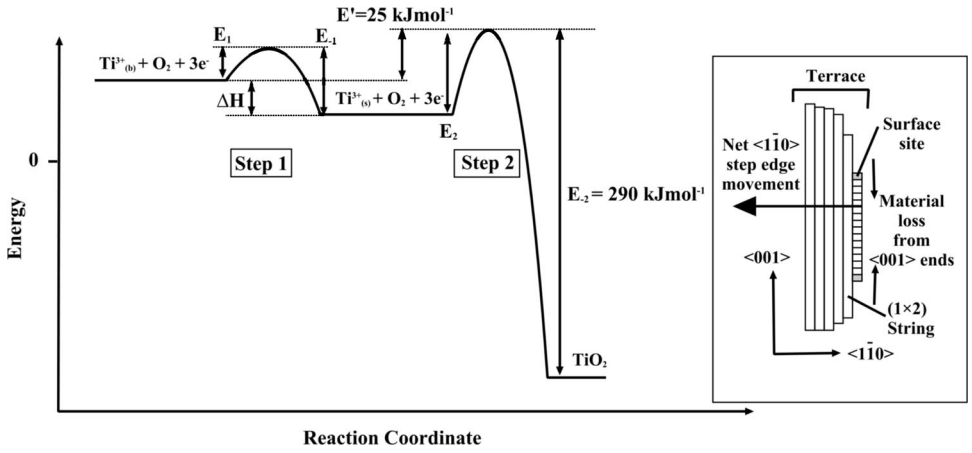

FIG. 7. A schematic reaction profile showing reactions (1) and (2). E' is the activation energy obtained from the Arrhenius plot in Fig. 6. Note that (*b*) denotes bulk and (*s*) denotes surface. The inset shows the model used for surface reduction at high temperatures ($T > \sim 1000$ K).

$$\ln\left(\frac{r}{P_{O_2}}\right) = \ln(27[\mathrm{Ti}^{3+}_{(b)}]^4 A') - \frac{E'}{RT}. \tag{11}$$

Hence, the value of E' may be obtained from the gradient of the plot of $\ln(r/P_{O_2})$ against $1/T$ in Fig. 6. As we shall see shortly, its value is so low because it is the sum of E_2 and ΔH.

We have previously observed that on heating TiO_2 to high temperature (1000 K) in the absence of oxygen in the STM it is possible to observe the step edges retreating across the surface.[12] We attribute this to the loss of O_2 into the gas phase and the dissolution of Ti into the bulk in interstitial form. The retraction of the steps occurred by a one-dimensional shortening of the most exposed (1×2) row (Fig. 7 inset). The rate of this retraction was found to be $\approx 0.021 \pm 0.006$ Å s^{-1} in the $\langle 001 \rangle$ direction. Given that one surface site in this direction on the surface is 2.96 Å in length, the rate of retraction (r') may be expressed as 7.09×10^{-3} sites s^{-1}. As the reaction is one dimensional, the concentration of sites [*s*] is always one per row. Using an Arrhenius-type expression, this information allows us to make an estimate of the activation energy for the reverse of the reoxidation reaction, given an assumed exponential prefactor of 10^{13} s^{-1}.

$$E_a = (\ln A + \ln[s] - \ln r')RT. \tag{12}$$

The value for E_a calculated by this method is 290 kJ mol^{-1}. This value is very high for an activation barrier, so it is easy to see why the reduction reaction requires such a high temperature to occur at an appreciable rate. The slow rate for this process at low temperatures is confirmed by substituting a lower temperature into Eq. (12). A temperature of 673 K gives a rate constant of $\sim 3\times10^{-10}$ s^{-1}, a negligible rate. Even at 1000 K the rate of oxygen desorption is so slow that it does not significantly affect the reoxidation rate measurements. The rate of surface reduction at a given temperature is dependent on the stoichiometry of the crystal. The crystal used to measure the activation energy for reduction was significantly reduced with a cross-linked (1×2) surface and evidence of shear plane formation.

Figure 7 shows a schematic reaction profile for the first two reaction steps. The figure shows why the observed energy from the Arrhenius plot, E', is so low. If ΔH is negative and smaller in magnitude than E_2, then the observed activation energy is small and positive. Given that there is no way to measure ΔH in the STM, it is not possible to calculate the true value of E_2.

Diebold *et al.* have carried out ^{18}O uptake measurements on TiO_2 (110) using SSIMS and obtained an activation energy of 19 kcal mol^{-1} ($\sim$80 kJ mol^{-1}).[17] This value is over three times larger than the value obtained in our study using STM. In contrast to our data, the Arrhenius plot in this paper is not linear for the whole temperature range. The linear region of the uptake rate data that are used to calculate the activation energy lies at temperatures from 477 to 530 K. At temperatures below 573 K the observed growth rate of new TiO_2 in our STM studies becomes very slow. Within the time scale of an STM experiment it is very difficult to observe more than a monolayer of growth. Some other oxygen adsorption process may be occurring in this lower-temperature regime that is not seen in the STM and does not result in the growth of new TiO_2 layers. Alternatively, it is possible that the bulk reduction level of the crystals is different in the two studies. This could result from different annealing temperatures: 950 K in the Diebold study as opposed to 1173 K in our study. It is therefore, not possible to make a direct comparison between the value obtained in this study and that obtained by Diebold *et al.*

V. CONCLUSIONS

By measuring the area of growth from many successive STM images, we have shown that the rate of surface growth of TiO_2 during reoxidation is first order in molecular oxygen pressure. The rate of reaction at constant pressure for five different temperatures has been calculated and plotted on an Arrhenius plot to yield an activation energy for the reaction of $25(\pm4)$ kJ mol^{-1}. We propose a mechanism for reoxidation whereby interstitial Ti^{3+} diffuses from the bulk to the

surface and is captured by gas-phase O_2 to form individual mobile TiO_2 units. This unit may then become incorporated into a step edge, or further TiO_2 units may be added to it to form added row (1×2). The growth process continues indefinitely in cycles of (1×1) and (1×2) growth, and during the period of the longest experiments the supply of interstitial Ti^{3+} was never exhausted.

ACKNOWLEDGMENTS

R.S. would like to thank the EPSRC and Johnson Matthey for financial support. R.B. would also like to thank the EPSRC for funding. Additionally, R.S. would like to thank Dr. C. L. Pang for helpful discussions and provision of Fig. 3.

*Corresponding author. FAX: +44 (0)118 9316331. Email address: m.bowker@reading.ac.uk

[1] A. Dickinson, D. James, N. Perkins, T. Cassidy, and M. Bowker, J. Mol. Catal. A: Chem. **146**, 211 (1999).
[2] M. Grätzel, Cattech **3**, 4 (1999).
[3] H. Onishi and Y. Iwasawa, Surf. Sci. **313**, L783 (1994).
[4] C. L. Pang, S. A. Haycock, H. Raza, P. W. Murray, G. Thornton, O. Gülseren, R. James, and D. W. Bullett, Phys. Rev. B **58**, 1586 (1998).
[5] R. A. Bennett, S. Poulston, P. Stone, and M. Bowker, Phys. Rev. B **59**, 10 341 (1999).
[6] M. A. Henderson, J. Phys. Chem. B **101**, 221 (1997).
[7] R. A. Bennett, P. Stone, R. D. Smith, and M. Bowker, Surf. Sci. **454**, 390 (2000).
[8] E. L. D. Hebenstreit, W. Hebenstreit, and U. Diebold, Surf. Sci. **461**, 87 (2000).
[9] O. Dulub, W. Hebenstreit, and U. Diebold, Phys. Rev. Lett. **84**, 3646 (2000).
[10] F. Pesty, H. P. Steinruck, and T. E. Madey, Surf. Sci. **339**, 83 (1995).
[11] P. Stone, R. A. Bennett, and M. Bowker, New J. Phys. **1**, 8 (1999), www.njp.org
[12] R. A. Bennett, P. Stone, and M. Bowker, Faraday Discuss. **114**, 267 (1999).
[13] V. S. Lusvardi, M. A. Barteau, J. G. Chen, J. Eng, B. Frühberger, and A. Teplyakov, Surf. Sci. **397**, 237 (1998).
[14] Y. Yamaguchi, H. Onishi, and Y. Iwasawa, J. Chem. Soc., Faraday Trans. **91**, 1663 (1995).
[15] M. A. Henderson, Surf. Sci. **419**, 174 (1999).
[16] H. Zajonz, H. L. Meyerheim, T. Gloege, W. Moritz, and D. Wolf, Surf. Sci. **398**, 369 (1998).
[17] M. Li, W. Hebenstreit, L. Gross, U. Diebold, M. A. Henderson, D. R. Jennison, P. A. Schultz, and M. P. Sears, Surf. Sci. **437**, 173 (1999).
[18] C. Doornkamp, M. Clement, and V. Ponec, J. Catal. **182**, 390 (1999).
[19] M. Bowker, S. Poulston, R. A. Bennett, P. Stone, A. H. Jones, S. Haq, and P. Hollins, J. Mol. Catal. A: Chem. **131**, 185 (1998).
[20] M. Li, W. Hebenstreit, U. Diebold, A. M. Tyryshkin, M. K. Bowman, G. G. Dunham, and M. A. Henderson, J. Phys. Chem. B **104**, 4944 (2000).
[21] R. A. Bennett, P. Stone, N. J. Price, and M. Bowker, Phys. Rev. Lett. **82**, 3831 (1999).
[22] M. Ashino, Y. Sugawara, S. Morita, and M. Ishikawa, Phys. Rev. Lett. **86**, 4334 (2001).
[23] H. Onishi, K. Fukui, and Y. Iwasawa, Bull. Chem. Soc. Jpn. **68**, 2447 (1995).
[24] S. D. Elliott and S. P. Bates, Phys. Chem. Chem. Phys. **3**, 1954 (2001).
[25] Y. Iwasawa, H. Onishi, and K. Fukui, Topics in Catalysis **14**, 163 (2001).
[26] K. Ruebenbauer, U. D. Wdowik, M. Kwater, and J. T. Kowalik, Phys. Rev. B **54**, 12 880 (1996).
[27] H. Onishi and Y. Iwasawa, Phys. Rev. Lett. **76**, 791 (1996).
[28] F. Millot, J. Mater. Sci. Lett. **4**, 902 (1985).
[29] R. A. Bennett and A. J. Ramirez-Cuesta (unpublished).
[30] A. J. Ramirez-Cuesta, R. A. Bennett, P. Stone, P. C. H. Mitchell, and M. Bowker, J. Mol. Catal. A: Chem. **167**, 171 (2001).